Chemical Engineering Journal 102 (2004) 25–33

Chemical Engineering Journal

www.elsevier.com/locate/cej

A study on intermittency phenomena in the impeller stream via digital particle image velocimetry (DPIV)

Jianhua Fan, Yundong Wang*, Qi Rao, Weiyang Fei

The State Key Laboratory of Chemical Engineering, Department of Chemical Engineering, Tsinghua University, Beijing 100084, PR China

Received 27 October 2003; accepted 5 February 2004

Abstract

To characterize intermittency phenomena in the impeller jet, digital particle image velocimetry (DPIV) was used to measure the near-instantaneous flow fields in baffled, stirred reactor, equipped with a Rushton turbine (RT) impeller of large impeller and reactor diameter ratio. From the transient velocity fields obtained by DPIV, characterized by a chaotic movement of the jet axis in a fan section in the plane of laser sheet, effective intermittency phenomena in the impeller stream were identified for lower rotational speed. To gain insight into the nature of the intermittency phenomena, the impeller discharge angle corresponding to the near-instantaneous velocity field was calculated and its time series were constructed and analyzed via frequency count and power spectral density function (PSD). The macro-instability (MI) behavior of the reactor was investigated and its presence in the bulk flow was verified via spectral analysis of time series of the spatially averaged vorticity for lower rotational speed (namely 30, 60 and 120 min^{-1}). Coherent spectral analysis was introduced to determine the cause of the intermittency phenomenon in the impeller stream as well as the relationship between the intermittency phenomenon and MI in the bulk flow. Results show that intermittency in the impeller stream is linearly related to MI in the reactor. The influence of MI should not be neglected in study of impeller stream intermittency phenomena.

Keywords: Stirred reactor; Intermittency in the impeller stream; Macro-instability (MI); Digital particle image velocimetry (DPIV); Spatially averaged vorticity; Coherent spectral analysis

1. Introduction

Stirred-tank reactors, mechanically agitated by one or more impellers, are among the most widely used reactors in chemical and allied industries. The rotation of impellers generates extremely complex flow within the stirred vessel. Therefore, understanding fluid dynamic characteristics of the impeller discharge flow is essential for reliably design and scale-up of stirred reactors.

Various experimental and numerical studies have been done to characterize the complex fluid dynamics in the impeller discharge region. According to the measurement technique, these studies can be divided into two categories: angle-averaged and angle-resolved. For the angle-averaged study, the flow fields in the impeller region were obtained by averaging the instantaneous flow field over 360° of the impeller revolution. Most of those studies were carried out in the 1980s [1,2] and were reviewed by Ranade and Joshi [3]. Later in 1990s, several attempts had been made to measure angle-resolved flow characteristics in stirred tanks. Schaefer et al. [4], Lee and Yianneskis [5] investigated turbulence properties of the impeller stream induced by a RT impeller, using laser Doppler velocimetry (LDV). Comprehensive data of high spatial resolution were obtained through angle-resolved and time-resolved LDV measurement. The nature of the turbulence in the discharge stream was characterized. LDV were essentially a single point technique to measure the angle-averaged and angle-resolved flow characteristics. Instantaneous measurements of large-scale structure around rotating impeller blade are, therefore, impossible. Digital particle image velocimetry (DPIV), an instantaneous multiple-point measurement technique, was used recently to characterize flow structures near impeller blades.

Ranade et al. [6] studied the trailing vortices behind the blades of a Rushton turbine by DPIV. Both angle-resolved

Abbreviations: CCD, charge couple device; CFD, computational fluid dynamics; DPIV, digital particle image velocimetry; LDV, laser Doppler velocimetry; LES, large eddy simulation; LIF, laser induced fluorescence; MI, macro-instability; PBT, pitched blade turbine; POD, proper orthogonal decomposition; PSD, power spectral density; VTR, video tape recording; RT, Rushton turbine

* Corresponding author. Tel.: +86-10-627-827-48; fax: +86-10-627-703-04.
E-mail address: wangyd@tsinghua.edu.cn (Y. Wang).

1385-8947/$ – see front matter © 2004 Elsevier B.V. All rights reserved.
doi:10.1016/j.cej.2004.02.002

Nomenclature

a	blade width (m)
b	blade height (m)
C	clearance (m)
$C(\omega)$	coherent spectral function
D	impeller diameter (m)
f_{MI}	macro-instability frequency (s^{-1})
f'_{MI}	non-dimensional macro-instability frequency, $f'_{MI} = f_{MI}/N_I$
$h(\omega)$	power spectral density function
H	liquid height in reactor (m)
i, j	index for radial and axial direction, dimensionless
I, J	total index number for radial and axial direction, dimensionless
$I_{N,M}(\omega_k)$	the modified periodogram
k	index for discrete set of frequencies
M	length of time series after padding
n	flow field number in the time series, dimensionless
N	total number of flow fields
N_I	impeller rotational speed (s^{-1})
Re	impeller Reynolds number, $N_I D^2/v$
T	reactor diameter (m)
$u_{i,j,n}$, $v_{i,j,n}$	nth instantaneous velocity in the radial and axial direction, respectively ($m\,s^{-1}$)
$\bar{u}_d$,$\bar{v}_d$	spatially averaged radial and axial velocity component in the impeller region ($m\,s^{-1}$)
$\bar{u}_{i,j}$,$\bar{v}_{i,j}$	mean velocity in the radial and axial direction, respectively ($m\,s^{-1}$)
$w_{i,j,n}$	vorticity (s^{-1})
$\bar{w}_n$	spatially averaged vorticity (s^{-1})
W	baffle width (m)
W_B	modified Bartlett window function
x, y	distance for radial and axial direction (m)
Greek letters	
ϕ	impeller discharge angle (rad)
ω	frequency ($rad\,s^{-1}$)
ω_k	discrete set of frequencies

and angle-averaged flow fields near the impeller blades were obtained. The trailing vortices were further investigated numerically using commercial CFD code, Fluent. A satisfactory agreement was achieved among experimental data, published data and numerical simulation. Sharp and Adrian [7] studied the instantaneous flow structure in a region surrounding the blade tip of a Rushton turbine mixer using DPIV. The impeller stream jet and tip vortices in the transient flow fields were reported to be considerably unstable. Similar jet flow instability was also recognized by Houcine et al. [8], who investigated the feed stream jet intermittency phenomenon in a continuous stirred-tank reactor via instantaneous digital laser induced fluorescence (LIF) measurement. As will be discussed later in this work, the occurrence of unsteadiness in the impeller region might be partly due to the influence of large-scale flow instabilities in the bulk flow. Those large-scale flow instabilities were first detected by Winardi and Nagase [9] in a mixing vessel with a marine propeller using flow visualization and LDV techniques, and then identified as MI by Bruha et al. [10] using a mechanical device, called "tornado meter". Characterized by space and time scale considerably exceeding the scales of turbulence eddies, MI was reported to represent not only flow pattern alternation but a significant influence on the mixing process [11], the local heat [12] or mass fluxes and local gas or solid holdup for two-phase flow [13]. Therefore, various experimental studies had been carried out to gain understanding of mechanisms of the MI formation and development as well as its properties. At early stage, studies on MI were observational measurements, via flow visualization techniques such as visual observation, high speed video tape recording (VTR), video recording, LDV [9] and tuft flow visualization [14]. Investigations of MI phenomena are effective with the use of different tools in signal processing, particularly with spectral analysis [15–17], proper orthogonal decomposition (POD) [18], velocity decomposition technique [19] and probability analysis [20]. The macro-instabilities in stirred vessel were also investigated by Myers et al. [21] and Fan et al. [20], via two-dimensional DPIV measurement. Large eddy simulation (LES) was also implemented to provide data throughout the tank at each instant time to investigate large-scale chaotic structures in stirred tank [22–24], although the work is computationally intensive and presently not viable for design and development purposes.

The objective of this work is to characterize the intermittency phenomenon in the impeller jet and to further investigate the influence of turbulent macro-instability on the discharge stream. The transient two-dimensional velocity fields of the vertical mid-plane between baffles, in baffled stirred tank equipped with a Rushton turbine impeller, were measured using DPIV. The discharge angle corresponding to the near-instantaneous flow field was calculated. Time series of the discharge angle was constructed and investigated via frequency count and spectral analysis, to gain insight into the nature of the intermittency phenomenon in the impeller stream. Macro-instability behavior of the reactor was investigated via spatially averaged vorticity. The cause of the impeller stream intermittency phenomenon and its relationship with MI in the bulk flow, were determined by coherent spectral analysis.

2. Experimental

The DPIV apparatus used in this study is FlowMap 1500 system from Dantec Measurement Technology. The flow was seeded with polyamid seeding particles of 20 μm diameter and of 1030 $kg\,m^{-3}$ density. Up to 20 Hz pulsed

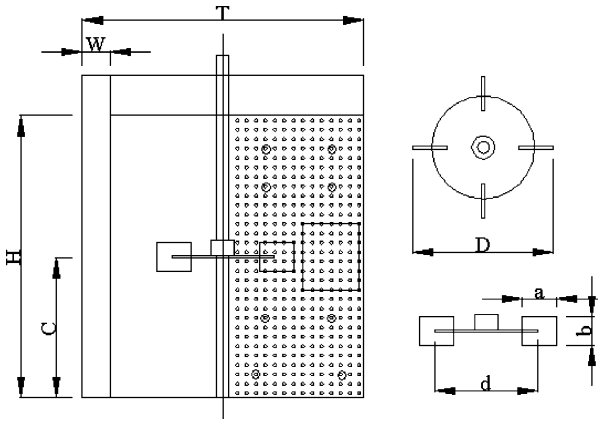

Fig. 1. Stirred vessel configuration, impeller geometry and location of experimental point (the impeller region is defined as area bordered by the square and location of the points for study of MI are represented as hollow circles).

Nd:Yag laser with a beam expanding lens was used to create a light sheet of 10 mm thickness to illuminate the measurement area. A Nikon Hisence CCD camera was placed at the right angle to the light sheet to record images with resolution of 1280 × 604 pixels. The recorded images were divided into interrogation area of 64 × 64 pixels with a 50% overlap, resulting approximately 660 vectors for the entire vessel. The average relative error for the near-instantaneous velocity measurement was 0.625%.

The DPIV experiments were carried out in a cylindrical Perspex vessel. The configuration of the reactor is shown in Fig. 1. The reactor diameter $T = 0.28$ m, equipped with four baffles (width $W = T/10$, 90° apart) and filled with water of a height up to $H = T$. The fluid is stirred by a four-blade Rushton turbine (diameter $D = T/2$, blade height $b = D/5$, blade width $a = D/4$). The impeller clearance, C, is fixed at $T/2$. To minimize the effect of vessel curvature on the intersecting beams and thus on the optical distortion, the whole reactor was submerged into a square glass tank, which was filled with the same working fluids. The measurement area was vertical mid-plane between adjacent baffles. In this experiment, the density and viscosity of water are 998 kg m^{-3} and 1.0 mPa s, respectively and the impeller was driven at the speed of 30, 60, 120 and 180 min^{-1}, respectively.

In the study of MI via spectral analysis, the number of sample data and the resulting sample time were important parameters to guarantee measurement accuracy. The increase of the total number of sample data and thus the sample time will increase the measurement accuracy. However, this will raise running cost at the same time. To keep the balance between measurement accuracy and running cost, 1024 successive DPIV measurements were carried out using a time delay of about 0.5 ms, resulting a measurement period of approximately 8.8 min for a sampling rate 2 s^{-1}. Previous experiment showed that this sampling rate (2 s^{-1}) was fast enough to capture the fastest MI transient observed in the present reactor [20].

3. Data processing

To identify and characterize flow instabilities in the impeller region, after treatment of the near-instantaneous velocity fields acquired from DPIV measurement were performed. The data reprocessing procedure includes calculation of time averaged velocity field, calculation of inclination angle and the spatially averaged vorticity, construction and subsequently spectral analysis of time series of the inclination angle and the spatially averaged vorticity.

The time averaged velocity field was calculated in Eq. (1), where u and v denote radial and axial velocity component, respectively; i and j are position index in radial and axial direction; n denotes the nth transient flow field in the time series and N is the total number of near-instantaneous flow fields obtained:

$$\bar{u}_{i,j} = \frac{1}{N}\sum_{n=1}^{N} u_{i,j,n}, \qquad \bar{v}_{i,j} = \frac{1}{N}\sum_{n=1}^{N} v_{i,j,n} \tag{1}$$

The inclination angle of the impeller discharge stream was defined in Eq. (2):

$$\phi = \arctan\left(\frac{\bar{v}_{\mathrm{d}}}{\bar{u}_{\mathrm{d}}}\right) \tag{2}$$

where $\bar{v}_{\mathrm{d}}$ and $\bar{u}_{\mathrm{d}}$ denote the spatially averaged axial and radial velocity in the impeller region, respectively. The impeller region location is shown in Fig. 1. This definition of the inclination angle, via spatially averaged velocity, may not precisely represent the actual deflection of flow direction, but will not significantly influence the final conclusion we draw. As the main objective of the present work is to study the large-scale flow structure, the instantaneous velocity field was filtered by a 5 × 5 filter before calculation of inclination angle, so as to average out noise from the small turbulence eddies.

To characterize the asymmetry of flow circulation in the measurement plane, spatially averaged vorticity corresponding to the nth velocity field, $\bar{w}_n$, was introduced and defined as follows, Eq. (3):

$$\bar{w}_n = \frac{1}{I \times J}\sum_{i=1}^{I}\sum_{j=1}^{J} w_{i,j,n} \tag{3}$$

where $w_{i,j,n}$ denotes Z-component of the nth vorticity for point i, j corresponding to the nth velocity field. $w_{i,j,n}$ can be calculated from discrete velocity fields using finite difference approximations of the derivatives, Eq. (4). Sensitive to the overall flow alternation in the bulk flow, the spatially averaged vorticity can be used to investigate the MI phenomena, which was verified by Myers et al. [21]:

$$w_{i,j,n} = \frac{\partial v_{i,j,n}}{\partial x} - \frac{\partial u_{i,j,n}}{\partial y} \tag{4}$$

The time series of the inclination angle and the spatially averaged vorticity were constructed by performing the same

calculation over all the 1024 sequential near-instantaneous velocity fields. As will be seen in Fig. 4, the signal looks so random that it is difficult to extract any information from the time series. In present work, the power spectral density function $h(\omega)$, calculated using the discrete Fourier transform after applying a modified Bartlett window (with a window parameter of 50), was introduced to investigate the behavior of MI, Eq. (5). These algorithms were described in detail by Priestley [25]:

$$h(\omega) = \frac{2\pi}{M} \sum_{k=-M/2}^{M/2} I_{N,M}(\omega_k) W_B(\omega - \omega_k) \quad (5)$$

To investigate relationship between intermittency in the impeller stream and the macro-instability in the bulk flow, coherent spectrum function $C(\omega)$ (at frequency ω) was introduced and defined as Eq. (6),

$$C_{12}(\omega) = \frac{h_{12}(\omega)}{\{h_{11}(\omega)h_{22}(\omega)\}^{1/2}} \quad (6)$$

where series 1 and 2 denote time records of the spatially averaged vorticity and inclination angle, respectively; $h_{11}(\omega)$ and $h_{22}(\omega)$ are the non-normalized auto-spectrum for series 1 and 2, respectively, and $h_{12}(\omega)$ is the non-normalized cross-spectrum between series 1 and 2. The definition of $h_{12}(\omega)$ is similar to that of $h_{11}(\omega)$ and $h_{22}(\omega)$, and is described in detail by Priestley [25].

All computations were computer-programmed and performed on a Fortran 90 platform. Detailed information can be found in a book written by Press et al. [26].

4. Results and discussion

4.1. Flow pattern instability

The time-averaged velocity field in the vertical mid-plane between adjacent baffles, obtained by averaging the sequential 1024 DPIV measurement, is illustrated in Fig. 2. An apparent symmetric double loop flow pattern is observed. The jet flow coming off the impeller blades streams towards the wall and is divided into two flows under the influence of the vessel wall: one flow downwards along the wall, to the bottom of the vessel, then back to the impeller region. The others rise along the wall, to the top of the vessel and back to the impeller region, forming a symmetric double loop. Similar flow patterns have been reported by Costes and Couderc [27].

Generally, such a double circulation loop pattern was thought to fill the entire vessel. In contrast to this simple picture, flow fields in a stirred tank are rather complex and unstable. The randomly captured near-instantaneous flow fields are presented in Fig. 3. The instantaneous flow fields, substantially complex and stochastic, are different to the mean velocity field. Conventional double loop flow pattern

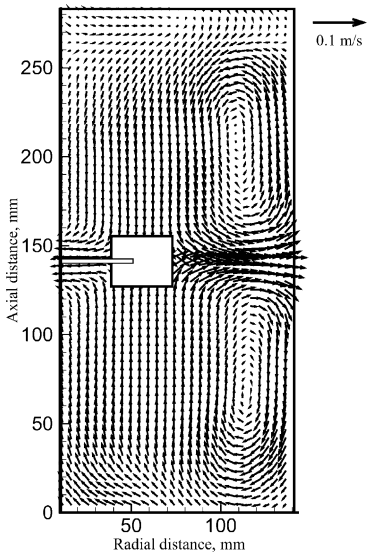

Fig. 2. Mean velocity field of vertical mid-plane between adjacent baffles ($D/T = 0.5$, $C/T = 0.5$, $N_I = 30\,\text{min}^{-1}$, $Re = 9780$).

is scarcely observed, rather, a large-scale unstable circulation pattern dominates the entire tank. These large-scale flow instabilities have been recognized by many scholars, including Winardi and Nagase [9] who identified flow instabilities via high speed VTR, Chapple and Kresta [14] via tuft flow visualization, and Montes et al. [15] via flow visualization technique. DPIV technique can eliminate personal errors and inaccuracy due to its high resolution and capacity to capture time varying flow fields.

To study flow pattern instability, vorticity was introduced to characterize the rotation of fluid elements. As seen in Fig. 3(c) and (d), the discharge flow, which turns upwards under the influence of vessel wall, rotates counterclockwise, and therefore gives a positive vorticity. Conversely, the discharge stream, which flows downwards, rotates clockwise and gives a negative vorticity. For the measurement plane, the vorticity was further spatially averaged to characterize the asymmetry of the transient flow fields. Fig. 3(a) shows a near-instantaneous velocity field with a negative spatially averaged vorticity, where large region of negative vorticity in the lower part of the measurement plane dominates the small region of positive vorticity in the upper part. For a near-instantaneous velocity field, where large region of positive vorticity in the upper part of the measurement plane dominates the small region of negative vorticity in the lower part (Fig. 3(b)), the spatially averaged vorticity is positive. The near-instantaneous flow field is nearly symmetric while the spatially averaged vorticity is approximately zero.

Fig. 4 shows time series of the spatially averaged vorticity. The signal is rather random and stochastic, with the values fluctuating between -0.2 and $0.2\,\text{s}^{-1}$. This indicates the presence of dominant asymmetric circulation flow, with direction and strength of rotation changing with time. The agreement of the spatially averaged vorticity with the transient velocity fields verifies the use of the spatially averaged

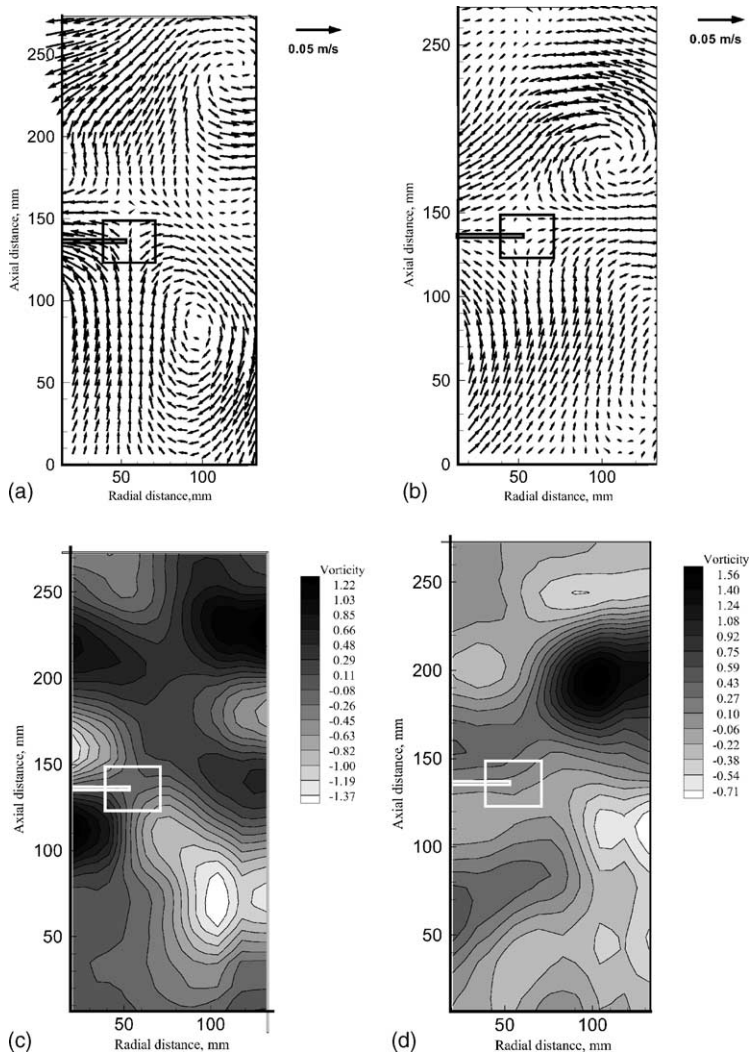

Fig. 3. Near-instantaneous velocity fields showing inclination of the impeller discharge stream (a) and (c) at time 32.5 s having a discharge angle of -34° and a spatially averaged vorticity of $-0.06\,s^{-1}$, (b) and (d) at time 57.0 s having a discharge angle of 6° and a spatially averaged vorticity of $0.03\,s^{-1}$ ($D/T = 0.5$, $C/T = 0.5$, $N_1 = 30\,min^{-1}$, $Re = 9780$).

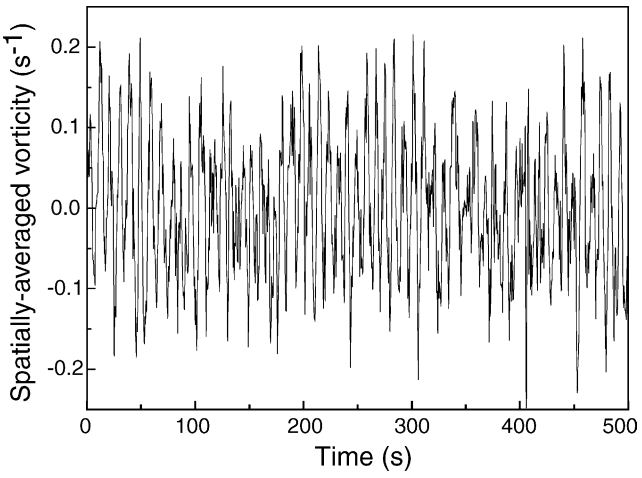

Fig. 4. Time series of the spatially averaged vorticity.

vorticity to characterize flow macro-instability in a stirred tank, which had also been successfully implemented by Myers et al. [21] in their study of MI with a pitched-blade turbine (PBT) tank.

To further investigate time records of the spatially averaged vorticity, the power spectral density (PSD) estimate at frequency 0–1.0 s^{-1} was calculated (Fig. 5). For a rotational speed of 30 min^{-1}, a well-defined peak can be found at frequency 0.11 s^{-1}. To make sure that this dominant frequency is corresponding to MI, time records of axial and radial velocity at several points were investigated via spectral analysis (location of those points was shown as hollow circles in Fig. 1). A well-defined peak can be observed at the same frequency (0.11 s^{-1}) for all the PSD spectra studied. Owing to the fact that these low-frequency fluctuations in the vorticity signal is similar to MI found by many authors [10,15,17,21,24], these fluctuations can be taken as the

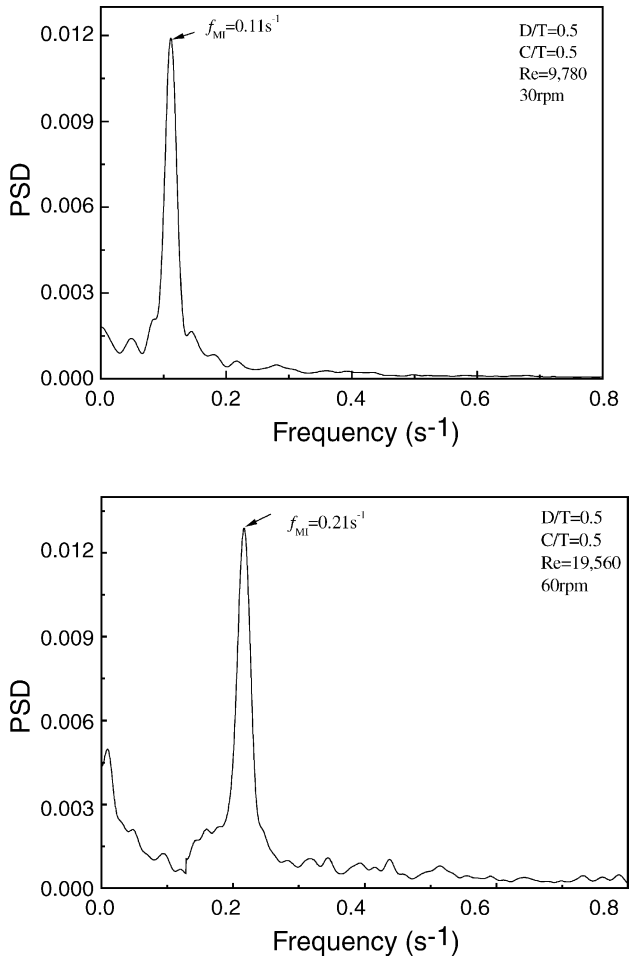

Fig. 5. Power spectral density of the time record of the spatially averaged vorticity showing macro-instability phenomenon.

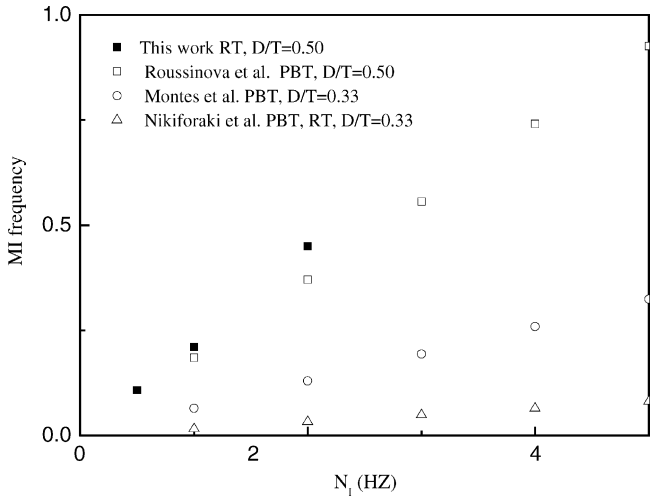

Fig. 6. Comparison of the MI frequency variation with impeller speed obtained in different studies.

signature of existence of MI phenomena. To study the variation of f_{MI} with N_I, MI behavior at 60, 120 and 180 min^{-1} were also studied. Results show that dominant frequencies corresponding to MI can be observed for lower rotational speed (namely 30, 60 and 120 min^{-1}). When we study PSD spectra for 180 min^{-1}, the spectra looks more random and stochastic, with many poorly defined peaks. PSD spectra of the axial and radial velocity signal also revealed none pronounced frequencies corresponding to MI. The variation of f_{MI} with N_I was investigated and plotted in Fig. 6. For the present study, the non-dimensional MI frequency f'_{MI} gives 0.22. Those findings were different with those reported by Nikiforaki et al. [17] and Montes et al. [15], but similar to the results reported by Roussinova et al. [24]. Nikiforaki et al. [17] found that f'_{MI} keeps in the range of 0.015–0.02 for their PBT/RT study. Compared with that of Nikiforaki et al. [17], Montes et al. [15] got a value a little higher (0.06) for their study with PBT tank. Roussinova et al. [24] reported that the dimensionless frequency of MI remains constant at 0.186 for their study of PBT tank with impeller diameter $D = T/2$. The discrepancy between those studies may be partly due to the influence of impeller-to-tank diameter ratio and impeller type. The PBT/RT impellers used by Montes et al. [15] and Nikiforaki et al. [17] have a impeller-to-tank diameter ratio (D/T) of 0.33, while for the present work and work of Roussinova et al. [24] the ratio is 0.5. The disagreement of MI frequency between different studies was also addressed and further investigated by Nikiforaki et al. [17], who reported that the total measurement time and logarithmic analytical method may also affect the selection of appropriate frequency corresponding to MI. Although many works had been done in the literature to characterize MI in stirred reactor, the origin and nature of MI are still not well understood and a more detailed investigation of MI behavior is necessary for further study [17].

4.2. Intermittency phenomena in the impeller discharge stream

When we observe flow in the impeller region, the jet oscillates in the plane of the laser sheet. When the circulation flow in the lower part of the reactor is energetic enough, the impeller discharge stream is entrained downwards and backs to reinforce the circulation flow. This yields a negative discharge angle (Fig. 3(a)). When the circulation flow in the upper part of the reactor is more powerful, the impeller discharge steam is entrained upwards, yielding a positive discharge angle (Fig. 3(b)). While the circulation flow in the lower part counterbalances that in the upper part, the stream jet axis is almost horizontal, giving a discharge angle close to zero.

The impeller discharge angle, as defined in Eq. (2), was calculated and its time series was constructed. The results were presented in Fig. 7. As observed in the instantaneous velocity fields, the discharge angle was not fixed at zero. It fluctuated dramatically with time, with some fluctuations exceeding the range of -50° to 50°. Because the randomly fluctuating signal makes it difficult to extract information

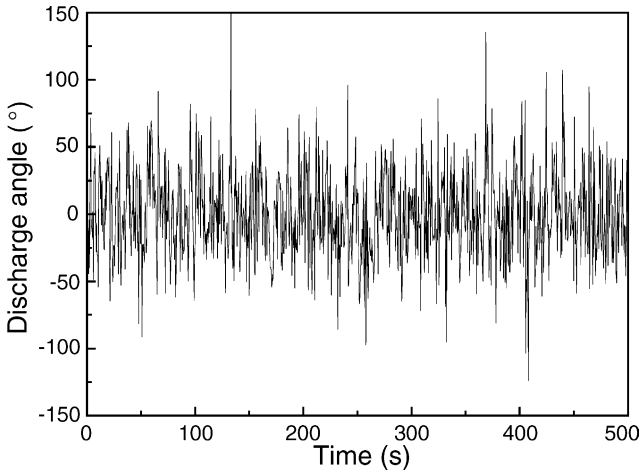

Fig. 7. Time series of the inclination angle of impeller discharge stream.

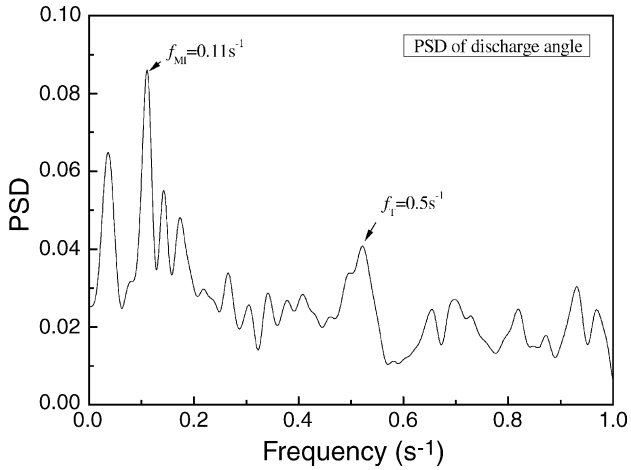

Fig. 9. Power spectral density of the time record of the inclination angle ($D/T = 0.5$, $C/T = 0.5$, $N_I = 30\,\text{min}^{-1}$, $Re = 9780$).

from the time series, the frequency count was used to describe statistic characteristics of the time records. The distribution and frequency of the inclination angle is presented in Fig. 8, with the step increment for the inclination angle equal to 10°. The plot of the frequency count versus the discharge angle obeys the normal distribution law, with approximately 50% of the total count falling between −20° to 25° and 90% between −50° to 55°. This gives evidence of the presence of effective intermittency characterized by a chaotic movement of the jet axis in a fan section in the plane of laser sheet, with the upper and lower bound 50° from the horizontal line.

4.3. Relationship between the impeller stream intermittency and MI in the bulk flow

In order to further investigate random fluctuations of the discharge angle, power spectral density estimated at frequency between 0 and 1.0 s^{-1} was calculated and presented in Fig. 9. Compared with PSD of the spatially averaged vorticity, the PSD of the inclination angle looks more stochastic. However, a dominant frequency can still be observed at frequency of 0.11 s^{-1}, indicating the presence of harmonic fluctuations with occurrence frequency of 0.11 s^{-1}. This dominant frequency is at the same location as the frequency of MI (f_{MI}) in the PSD of the spatially averaged vorticity. We can deduce that the impeller discharge stream is subject to the influence of flow macro-instabilities in the reactor and the dominant harmonic fluctuation of the discharge angle is due to MI. In order to verify this deduction, relationship between the time series of the spatially averaged vorticity and the discharge angle was studied via coherent spectrum, which will be discussed later in detail. It is interesting to note the dominant frequency (0.5 s^{-1}) is equal to the impeller frequency in the present work (for a rotation speed of 30 min^{-1}). The maximum possible interpretation of this frequency is the impeller passage effect, which is different to Myers et al. [21] who reported that blade passage did not strongly influence flow instabilities in a PBT tank and Fan et al. [20] who found that the blade passage effect did not influence PSD of the vorticity. However, this is not contradictory, since the conclusion drawn by Myers et al. [21] and Fan et al. [20] is applied to the bulk flow. From these results, we can conclude that although the blade passage effect may not be significant in the bulk flow, it cannot be neglected for the study of flow dynamics and properties in the impeller region.

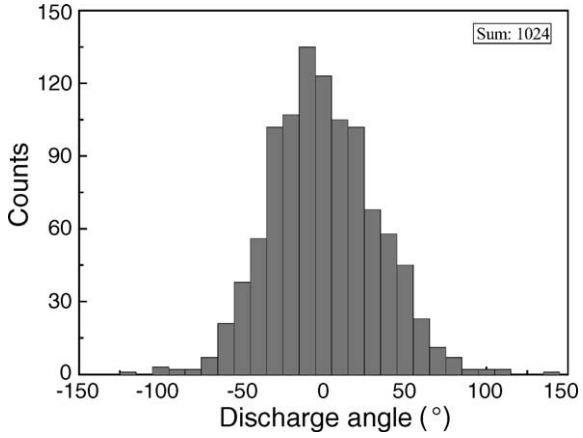

Fig. 8. Distribution of the inclination angle of the impeller stream for 8.5 min or 1024 counts ($D/T = 0.5$, $C/T = 0.5$, $N_I = 30\,\text{min}^{-1}$, $Re = 9780$).

Fig. 10 illustrates the coherent spectrum between time series of the spatially averaged vorticity and the inclination angle. When the frequency is greater than 0.2 s^{-1}, the coherent spectrums are more stochastic, with many weak pulsation waves, which indicate that the two series are not intensively linear coupled. Even at the impeller frequency of 0.5 s^{-1}, the two series have a coherency estimate of approximately 0.06, which gives a proof that the impeller passage effect does not significantly influence PSD of the spatially

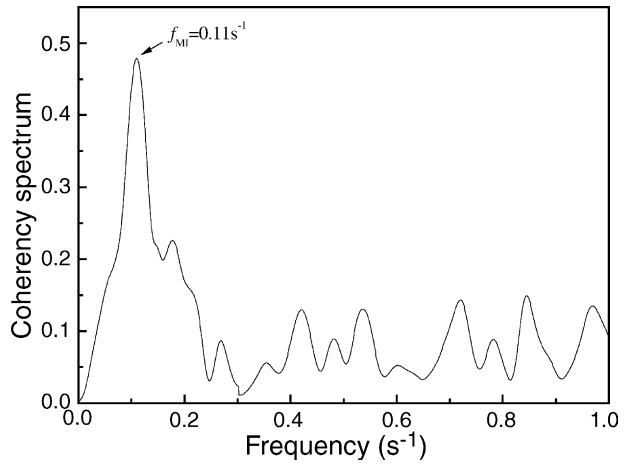

Fig. 10. Coherent spectrum between the time series of the spatially averaged vorticity and the inclination angle ($D/T = 0.5$, $C/T = 0.5$, $N_I = 30\,\text{min}^{-1}$, $Re = 9780$).

averaged vorticity despite that it has vital influence on the impeller discharge stream. At the frequency of $0.11\,\text{s}^{-1}$, the coherent spectrum shows a well-defined peak of 0.48, indicating that there is a fairly strong linear relationship between those two series. Explicitly, the intermittency in the impeller stream is linearly related to the large-scale low-frequency flow instability in the reactor and the occurrence of intermittency phenomena is partly due to MI in the reactor. When we study impeller stream intermittency for a rotation speed of $60\,\text{min}^{-1}$, similar result can be found. For higher rotational speed of $180\,\text{min}^{-1}$, the PSD spectra of the inclination angle series became more random, which made this analytical method inapplicable.

Similar feedstream jet intermittency phenomena in a continuous stirred-tank reactor were also studied by Houcine et al. [8], who identified the existence of feedstream jet intermittency phenomena and investigated the relationship between occurrence of intermittency and local characteristics of fluid flow. Their work mainly focuses on the dimensionless correlations characterizing intermittency occurrence. Results of the present work indicated that MI might have rather strong influence on the intermittency behavior of jet stream, therefore should not be neglected in study of impeller stream intermittency phenomena.

5. Conclusion

Based on the study of hydrodynamic instability by digital particle image velocimetry (DPIV), the intermittency phenomenon in the impeller stream jet and its relationship to macro-instability in the bulk flow have been described for rotational speed of 30, 60, 120 and $180\,\text{min}^{-1}$, respectively. From the near-instantaneous flow fields using DPIV, effective intermittency in the impeller stream was identified for lower rotational speed (30 and $60\,\text{min}^{-1}$). The impeller discharge angle was calculated and its time series were constructed. The frequency count of the angle fluctuations shows that the relationship between the frequency count and the inclination angle obeys the normal distribution law, with approximately 50% of the total fluctuations falling between the range of -20° to 25° and 90% falling between -50° to 55°. A harmonic process, corresponding to MI, was verified by spectral analysis of the random fluctuations of the discharge angle. Also in the PSD of the discharge angle, impeller passage effect manifests itself as a dominant frequency. Impeller passage effect cannot be neglected for the study of flow dynamic and properties in the impeller region although the blade passage effect may be not significant in the bulk flow.

Power spectral density of time series of the spatially averaged vorticity shows well defined peaks corresponding to MI for lower rotational speed (30, 60 and $120\,\text{min}^{-1}$). The dimensionless frequency f'_{MI} for the present work gives 0.22, which is different to those reported in the literature. The disagreement may be partly due to the difference in impeller-to-tank diameter ratio and impeller type used.

By means of coherent spectral analysis, the intermittency phenomenon in the impeller stream was found to be linearly related to macro-instability in the bulk flow. Therefore influence of MI should not be neglected in future study of impeller stream intermittency phenomena.

Acknowledgements

This research was carried out under Grant No. 29836130 of the National Natural Science Foundation of China, and Grant No. JZ2000080 of Tsinghua University Basic Research Fund, in the State Key Laboratory of Chemical Engineering of Tsinghua University, Beijing, PR China. The authors gratefully acknowledge these grants.

References

[1] K. Van't Riet, W. Bruijn, J.M. Smith, Real and pseudo-turbulence in the discharge stream from a Rushton turbine, Chem. Eng. Sci. 31 (6) (1976) 407–412.
[2] M. Yianneskis, M.Z. Popiolek, J.H. Whitelaw, An experimental study of the steady and unsteady flow characteristics of stirred reactors, J. Fluid Mech. 175 (1987) 537–555.
[3] V.V. Ranade, J.B. Joshi, Flow generated by a disc turbine. Part I. experimental, Trans. IChemE A 68 (1990) 19–33.
[4] M. Schaefer, M. Hoefken, F. Durst, Detailed LDV measurements for visualization of the flow field within a stirred tank reactor equipped with a Rushton turbine, Trans. IChemE A 75 (1997) 729–736.
[5] K.C. Lee, M. Yianneskis, Turbulence properties of the impeller stream of a Rushton turbine, AIChE J. 44 (1998) 13–24.
[6] V.V. Ranade, M. Perrard, N.L. Sauze, et al., Trailing vortices of Rushton turbine: PIV measurement and CFD simulation with snapshot approach, Trans. IChemE A 79 (2001) 3–12.

[7] K.V. Sharp, R.J. Adrian, PIV study of small scale flow structure around a Rushton impeller turbine, AIChE J. 47 (4) (2001) 766–778.
[8] I. Houcine, E. Plasari, R. David, J. Villermaux, Feedstream jet intermittency phenomenon in a continuous stirred tank reactor, Chem. Eng. J. 72 (1999) 19–29.
[9] S. Winardi, Y. Nagase, Unstable phenomenon of flow in a mixing vessel with a marine propeller, J. Chem. Eng. Jpn. 24 (2) (1991) 243–249.
[10] O. Bruha, I. Fort, P. Smolka, M. Jahoda, Experimental study of turbulent macro instabilities in an agitated system with axial high speed impeller and with radial baffles, Collect. Czech. Chem. Commun. 61 (1996) 856–867.
[11] F. Guillard, C. Tragardh, L. Fuchs, A study on the instability of coherent mixing structures in a continuously stirred tank, Chem. Eng. Sci. 55 (2000) 5657–5670.
[12] S. Hamm, R.S. Brodky, J.B. Fasano, Local heat transfer in a mixing vessel using the heat flux sensors, Ind. Eng. Chem. Res. 31 (5) (1992) 1384–1391.
[13] K.J. Bittorf, S.M. Kresta, Prediction of cloud height for solid suspensions in stirred tanks, in: Proceedings of the CHISA, Prague, Czech Republic, 2002, pp. 5–166.
[14] D. Chapple, S.M. Kresta, The effect of geometry on the stability of flow patterns in stirred tanks, Chem. Eng. Sci. 49 (21) (1994) 3651–3660.
[15] J.L. Montes, H.C. Boisson, I. Fort, M. Jahoda, Velocity field macro-instabilities in an axially agitated mixing vessel, Chem. Eng. J. 67 (1997) 139–145.
[16] C. Letellier, L.L. Sceller, G. Gouesbet, et al., Recovering deterministic behavior from experimental time series in mixing reactor, AIChE J. 43 (9) (1997) 2194–2202.
[17] L. Nikiforaki, G. Montante, K.C. Lee, M. Yianneskis, On the origin, Chem. Eng. Sci. 58 (2003) 2937–2949.
[18] P. Hasal, J.L. Montes, H.C. Boisson, I. Fort, Macro-instabilities of velocity field in stirred vessel: detection and analysis, Chem. Eng. Sci. 55 (2000) 391–401.
[19] V.T. Roussinova, B. Grgic, S.M. Kresta, Study of macro-instabilities in stirred tanks using a velocity decomposition technique, Trans. IChemE A 78 (2000) 1040–1052.
[20] J. Fan, Q. Rao, Y. Wang, W. Fei, Spatio-temporal analysis of macro-instability in a stirred vessel via digital particle image velocimetry (DPIV), Chem. Eng. Sci., in press.
[21] K.J. Myers, R.W. Ward, A. Bakker, A digital particle image velocimetry investigation of flow field instabilities of axial flow impeller, J. Fluids Eng. 119 (1997) 623–632.
[22] J. Revstedt, L. Fuchs, C. Tragardh, Large eddy simulation of the turbulent flow in a stirred reactor, Chem. Eng. Sci. 53 (24) (1998) 4041–4053.
[23] A. Bakker, L.M. Oshinowo, E.M. Marshall, The use of large eddy simulation to study stirred vessel hydrodynamics, in: Proceedings of the 10th European Conference on Mixing, Delft, The Netherlands, 2000, pp. 247–254.
[24] V. Roussinova, S.M. Kresta, R. Weetman, Low frequency macroinstabilities in a stirred tank: scale-up and prediction based on large eddy simulations, Chem. Eng. Sci. 58 (2003) 2297–2311.
[25] M.B. Priestley, Spectral Analysis and Time Series, Academic Press, New York, 1981.
[26] W.H. Press, S.A. Teukolsky, W.T. Vetterling, B.P. Flannery, Numerical Recipes in Fortran 77: The Art of Scientific Computing, Cambridge University Press, Cambridge, UK, 1992.
[27] J. Costes, J.P. Couderc, Study by laser Doppler anemometry of the turbulent flow induced by a Rushton turbine in a stirred tank: influence of the size of the units mean flow and turbulence, Chem. Eng. Sci. 43 (10) (1988) 2751–2764.